PHYSICAL REVIEW A, VOLUME 61, 041602(R)

Mach-Zehnder Bragg interferometer for a Bose-Einstein condensate

Yoshio Torii,* Yoichi Suzuki, Mikio Kozuma, Toshiaki Sugiura, and Takahiro Kuga
Institute of Physics, University of Tokyo, 3-8-1 Komaba, Meguro-ku, Tokyo 153-8902, Japan

Lu Deng and E. W. Hagley
National Institute of Standards and Technology, Gaithersburg, Maryland 20899
(Received 9 August 1999; published 28 February 2000)

We construct a Mach-Zehnder interferometer using Bose-Einstein condensed rubidium atoms and optical Bragg diffraction. In contrast to interferometers based on normal diffraction, where only a small percentage of the atoms contribute to the signal, our Bragg diffraction interferometer uses all the condensate atoms. The condensate coherence properties and high phase-space density result in an interference pattern of nearly 100% contrast. The two arms of the interferometer may be completely separated in space, making it an ideal tool that can be used to detect vortices or other topological condensate phases.

PACS number(s): 03.75.Fi, 03.75.Dg, 39.20.+q

With the advent of Bose-Einstein condensation (BEC) of dilute atomic gases [1,2] comes a coherent matter wave, or *atom laser* [3–5], analogous to an optical laser. The high phase-space density and coherence properties of condensates make possible atom-optic experiments that have previously only been performed with optical lasers, such as four-wave mixing [6]. Among these, atom-laser (matter-wave) interferometers [7,8] are of particular interest because of their potential high sensitivity. In order to be able to utilize atom lasers as one does optical lasers, atom-wave versions of optical elements, such as 50/50 beam splitters and mirrors, are needed. The recent demonstration of optical Bragg diffraction of a BEC by a moving, optical, standing wave [9] pointed the way toward the realization of that goal. Bragg diffraction efficiency can be varied from 0% to 100% by simply adjusting the Bragg-pulse duration and/or intensity [10,11]. This means that Bragg diffraction can function as an ideal, adjustable beam splitter/mirror for a BEC, providing us with the critical atom-optic elements needed for constructing an atom-laser interferometer. In this Rapid Communication we report a demonstration of a Mach-Zehnder interferometer for a BEC using an optical Bragg-diffraction technique. In addition to allowing alternative studies of the coherence properties of a BEC itself, such as vorticity [12], this interferometer may be used to measure phase coherence properties of potential matter-wave amplifiers.

Atom-wave interferometers comprised of optical standing waves can be classified into two types, those based on normal diffraction and those based on Bragg diffraction. In the case of normal diffraction there are many spurious momentum space paths, and only a small fraction of atoms ($\sim$10%) can contribute to the signal [13]. With Bragg diffraction, however, the atomic wave can be coherently split into only two paths, and then coherently recombined. This results in high efficiency [14] where, in principle, all of the atoms can contribute to the signal. Normal and Bragg diffraction based atom-wave interferometers were first demonstrated in 1995 using collimated metastable atomic beams, and fringe contrasts of 10% (normal) and 62% (Bragg) were obtained [13,14]. This is to be compared to our BEC Bragg-diffraction interferometer where all the atoms contribute to the signal due to the condensate's extremely narrow velocity spread [15]. Indeed, we achieve nearly the maximum contrast of 100% with a good single-shot visibility.

Bragg diffraction occurs when the atomic matter wave (a BEC nearly at rest) is coherently scattered by a moving, optical standing wave formed by counterpropagating laser beams of slightly different frequencies. The mechanism of Bragg diffraction can be most easily understood as a two-photon stimulated Raman process [9], where photons from one laser beam are coherently scattered into the other, changing the atomic momentum in the process. The frequency difference between the two counterpropagating Bragg beams is chosen to correspond to the energy difference between the two momentum states. In principle, the initial momentum state $|p=0\hbar k\rangle$ can be coupled to any momentum state $|p=2n\hbar k\rangle$ (n integer) using nth-order Bragg diffraction. In our case we choose to couple momentum states $|p=0\rangle$ and $|p=2\hbar k\rangle$ ($k=2\pi/\lambda$, and $\lambda=780$ nm is the laser wavelength). The momentum-space wave function of a condensate (initially in state $|p=0\rangle$) continuously irradiated with Bragg diffraction beams will oscillate between the two coupled momentum states just as if it were a two-level system. The effective oscillation frequency is $\Omega_{\text{eff}}=\Omega_1\Omega_2/2\Delta$, where Ω_1 and Ω_2 are the resonant Rabi frequencies of two Bragg beams, and Δ is the detuning of the beams from the optical transition [11,16]. As mentioned earlier, an arbitrary percentage of the atoms can be transferred to the $|p=2\hbar k\rangle$ momentum state by properly adjusting the intensity, detuning, and/or duration of the Bragg pulse.

In order to achieve 100% Bragg diffraction efficiency, the momentum spread of the condensate (δp) in the direction of Bragg momentum transfer must be much smaller than $\hbar k$. This condition arises because the Bragg pulse duration must be long enough to suppress normal diffraction. Lengthening the pulse reduces its Fourier width, thereby rendering the Bragg process more selective in momentum space [9]. Because we apply the Bragg beams along the axial (weak) di-

*Present address: Department of Physics, Gakushuin University, Mejiro 1-5-1, Toshima-ku, Tokyo 171-8588, Japan.

mension of our trap, the condition $\delta p \ll \hbar k$ is always well satisfied [17], allowing us to achieve 100% fringe contrast. In comparison, thermal beam interferometers satisfy such a condition by imposing tight constraints on the transverse collimation of the atomic beam. In this case, reduction of δp comes at the expense of atomic flux, resulting in a decrease of the signal-to-noise ratio.

The closed two-level system coupled by the Bragg beams can be most easily thought of as a fictitious spin-$\frac{1}{2}$ system, where we define $|g\rangle \equiv |p=0\hbar k\rangle$, and $|e\rangle \equiv |p=2\hbar k\rangle$. As usual, a $\pi/2$ (π) pulse is one that results in transferring half (all) of the atoms from $|g\rangle$ to $|e\rangle$. More precisely, the state vector of the system under a $\pi/2$ pulse obeys the transformation equations $|g\rangle \rightarrow (|g\rangle - e^{-i\varphi}|e\rangle)/\sqrt{2}$, and $|e\rangle \rightarrow (e^{+i\varphi}|g\rangle + |e\rangle)/\sqrt{2}$. Here φ is the phase of the moving standing wave in the center of the initial atomic wavepacket $|g\rangle$ in the middle of the Bragg pulse. Changes in φ are measured with respect to the phase of the resonant, moving standing wave. Successive application of this transformation shows that under a π pulse $|g\rangle \rightarrow -e^{-i\varphi}|e\rangle$, and $|e\rangle \rightarrow e^{+i\varphi}|g\rangle$. We can therefore use a $\pi/2$ (π) pulse as an ideal beam splitter (mirror) for the condensate.

We prepare a BEC of rubidium atoms using a dc magnetic trap and a standard evaporation strategy [1,18]. Briefly, we first trap about 10^9 ^{87}Rb atoms in an ultra-high-vacuum glass cell using a double magneto-optical trap [19]. The atoms are then transferred into a cloverleaf magnetic trap [17] and cooled using rf-induced evaporation. Every 5 minutes we create a BEC containing about 10^5 atoms in the $5S_{1/2}$ $F=1$, $m_F=-1$ state, in a trap with radial gradient, axial curvature, and bias field of 1.75 T/m, 185 T/m^2, and 10^{-4} T, respectively. Due to the geometry of our magnetic trap, the condensate is cigar shaped with the symmetry axis perpendicular to the direction of gravity. We release the condensate by suddenly switching off the magnetic trap within 200 μs, wait 5 ms for the mean-field driven explosive expansion to subside, and apply a Bragg interferometer pulse sequence. After 20 ms of free evolution to allow the $|g\rangle$ and $|e\rangle$ components enough time to separate significantly in space, an absorption image [1] of the resulting condensate is taken. This yields very clean and unambiguous signals since the action of the interferometer is mapped into the probability of observing atoms in two spatially separated regions.

The moving, optical standing wave is generated using two counterpropagating laser beams with parallel linear polarization but slightly different frequencies. These two laser beams are derived from a single diode laser using acousto-optic modulators, and the spatial mode of each beam is purified by passing through a single-mode fiber. The Gaussian beams are collimated, and have a full width at half maximum of $\sim$1 cm in order to minimize any spatial intensity gradient across the condensate. The light propagates parallel to the symmetry (long) axis of the trapped condensate, and the frequency difference between the two laser beams is $\delta/2\pi = 15$ KHz. This relative detuning corresponds to the two-photon recoil energy for rebidium mentioned earlier. Our laser intensities were chosen such that $\Omega_1/2\pi = \Omega_2/2\pi \cong 5$ MHz. To suppress spontaneous emission we used a detuning $\Delta/2\pi = 2.0$ GHz. These parameters result in an effective two-photon Rabi frequency of $\Omega_{\text{eff}}/2\pi \cong 6.3$ kHz.

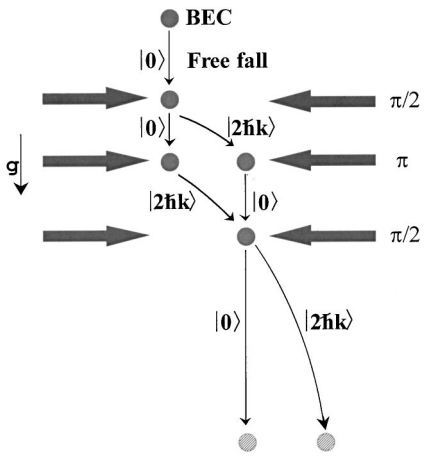

FIG. 1. Experimental schematic of the $\pi/2$-π-$\pi/2$ Mach-Zehnder Bragg interferometer.

The experimental schematic of our atom interferometer is shown in Fig. 1. The momentum-space condensate wave function Ψ, initially in state $|g\rangle$ ($|p=0\hbar k\rangle$), is coherently split by the first ($\pi/2$) pulse and becomes $\Psi_1 = (|g\rangle - |e\rangle)/\sqrt{2}$. Here, without the loss of generality, we have chosen $\varphi = 0$ (when $\varphi \neq 0$ there is an additional, physically meaningless, global phase multiplying the final wave function). In real space these two different momentum states begin to separate and, after a delay ΔT (measured from the center of successive Bragg pulses), the second (π) pulse is applied, producing $\Psi_2 = -(|g\rangle + |e\rangle)/\sqrt{2}$. Now the two spatially separated parts of Ψ_2 begin to converge because the action of the π pulse was effectively that of a mirror in momentum space. After another equal delay ΔT, the two parts of Ψ_2 from the two different coordinate-space paths overlap completely, and the third ($\pi/2$) pulse is applied yielding $\Psi_3 = -|g\rangle$. In this case the probability of finding the atoms in the initial state $|g\rangle$ after the sequence of three Bragg pulses is $P_g = |\langle \Psi_3 | g \rangle|^2 = 1$, regardless of the delay ΔT between the pulses. If, however, the phase of the moving, standing wave were altered by ϕ before applying the third Bragg pulse, $\Psi_3' = -[(1+e^{i\phi})|g\rangle + (1-e^{-i\phi})|e\rangle]/2$, and $P_g = [1+\cos(\phi)]/2$ ($P_e = [1-\cos(\phi)]/2$). Fringes in the final probability of observing atoms in the initial (or final) momentum state may therefore be mapped out by varying ϕ just before applying the final $\pi/2$ Bragg pulse.

The Bragg-pulse duration (for fixed Ω_{eff} and Δ) needed to produce a $\pi/2$ (π) pulse was first determined experimentally. Figures 2(a)–2(c) show absorption images of the condensate after applying a single Bragg pulse of duration $\tau = 0$, 40 ($\pi/2$ pulse), and 80 (π pulse) μs respectively. The condensate images are elliptical because of its initial anisotropic shape [1,18]. The experimentally determined durations are in excellent agreement with the calculated values of $\tau = 40$ μs and 80 μs based on the measured laser intensities and detuning. Once the $\pi/2$ (π) pulse durations were empirically determined, we proceeded with the actual interferometer experiment (Fig. 1) by applying the $\pi/2$-π-$\pi/2$ sequence of three

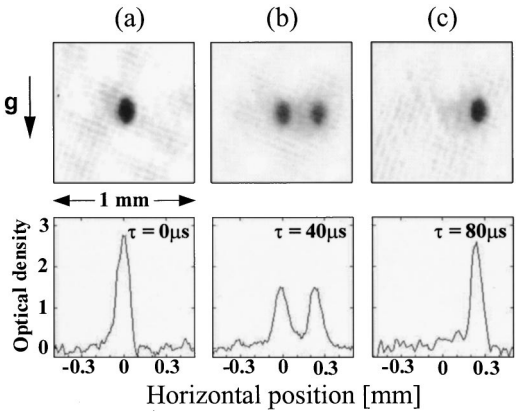

FIG. 2. Absorption images of the Bose condensate taken 20 ms after one Bragg pulse is applied (upper), and density profiles taken through the center of the condensates (lower), as a function of the pulse duration τ.

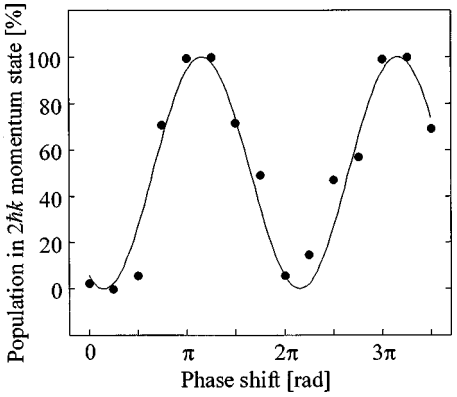

FIG. 3. Population oscillation of the condensate in the $|p=2\hbar k\rangle(|e\rangle)$ momentum state as a function of the phase shift ϕ of the third Bragg pulse. The time interval between the center of successive Bragg pulses is $\Delta T=190\ \mu$s.

Bragg pulses. The relative phase ϕ of the third $\pi/2$ pulse was experimentally adjusted in the range $0\leqslant\phi\leqslant 3.5\pi$ by changing the phase of one of the two Bragg beams comprising the moving standing wave with an electro-optic modulator (EOM).

Figure 3 shows the resultant oscillation of the population in the $|e\rangle$ state as a function of ϕ when $\Delta T=190\ \mu$s (each point represents a single measurement). Note that we observe an interference pattern with almost 100% contrast. This is to be compared to the best thermal beam interferometers for which the maximum contrast is only 62% [14]. Because the Bragg beams were not perfectly perpendicular to the direction of gravity, the falling condensates ''see'' a differential phase shift even when $\phi=0$. This results in the small $\sim 0.1\pi$ phase shift in the fringe pattern of Fig. 3. This phase shift corresponds to an angle misalignment of a few degrees from perpendicular, which is well within our experimental uncertainty.

The chosen pulse interval of 190 μs corresponds to a 2.2-μm separation of the two arms of the interferometer, or about six times the period of the optical standing wave made by the Bragg beams. Since the size of the condensate in the direction of momentum transfer is roughly 50 μm, $\Delta T>5$ ms is necessary to separate completely the two arms of the interferometer. However, we found that when $\Delta T>2$ ms, reproducibility of the interference pattern deteriorates significantly. When $\Delta T=3$ ms, the resulting fringe pattern is completely random, ranging from 0% to 100%. This indicates that the recombining wavepackets are fully coherent, even though their relative phase is not well controlled (this was also found to be true for $\Delta T>5$ ms). The phase stability of the Bragg beams was measured with a homodyne detection technique and was found to be shorter than 1 ms. This explains the lack of reproducibility at long ΔT and we suspect that the random relative phase is due to mechanical vibration of the numerous mirrors used for the Bragg beams. We believe that a stable signal contrast of 100% visibility can be achieved at long ΔT by actively stabilizing these critical Bragg mirrors. This would result in a stable interferometer whose two arms could be completely separated in space.

The Bragg interferometer presented here is an alternative tool that can be used to study phase properties of condensates. Although we demonstrated this Mach-Zehnder interferometer for a nontrapped BEC, the same method can be applied to trapped BECs [9]. For example, it should be possible to detect the phase signature of a vortex [12] in a trapped Bose-Einstein condensate using a slightly modified version of this interferometer. A vortex state could be created in the nondiffracted interferometer arm after the two momentum components spatially separate. The diffracted component, serving as a phase reference, would then be brought back to, and interfered with, the vortex state using an appropriate choice of Bragg pulses. The probability of finding atoms in the two output ports of the interferometer would be a momentum-space map of the condensate phase that can be analyzed with conventional imaging techniques [1]. Because a vortex has a characteristic azimuthally varying phase (0 to 2π), shot-to-shot global interferometer phase variations would not obscure the vortex phase signature (they would only cause a physical rotation of the interferometric images).

In addition to studying fundamental properties of condensates, such a BEC interferometer can be used to examine the coherence properties of potential matter-wave amplifiers [20]. For example, a small Bragg ''seed'' matter wave can be amplified to 50% of the initial condensate population using the recently demonstrated superradiance effect [21]. This amplified wave can then be used as the first ''$\pi/2$'' pulse in a three-pulse interferometer sequence, allowing one to check if the phase of the amplified matter wave is coherent with the seed that created it [22].

This work has been supported by a Grant-in-Aid from the Ministry of Education, Science, and Culture, as well as by Core Research for Evolutionary Science and Technology (CREST) of the Japan Science and Technology Corporation (JST).

[1] M. H. Anderson, J. R. Ensher, M. R. Matthews, C. E. Wieman, and E. A. Cornell, Science **269**, 198 (1995).

[2] K. B. Davis, M.-O. Mewes, M. R. Andrews, N. J. van Druten, D. S. Durfee, D. M. Kurn, and W. Ketterle, Phys. Rev. Lett. **75**, 3969 (1995).

[3] M.-O. Mewes, M. R. Andrews, D. M. Kurn, D. S. Durfee, C. G. Townsend, and W. Ketterle, Phys. Rev. Lett. **78**, 582 (1997).

[4] I. Bloch, T. W. Hänsch, and T. Esslinger, Phys. Rev. Lett. **82**, 3008 (1999).

[5] E. W. Hagley, L. Deng, M. Kozuma, J. Wen, K. Helmerson, S. L. Rolston, and W. D. Phillips, Science **283**, 1706 (1999).

[6] L. Deng, E. W. Hagley, J. Wen, M. Trippenbach, Y. Band, P. S. Julienne, J. E. Simsarian, K. Helmerson, S. L. Rolston, and W. D. Phillips, Nature (London) **398**, 218 (1999).

[7] *Atom Interferometry*, edited by P. R. Berman (Academic Press, Cambridge, 1997).

[8] D. E. Pritchard and P. L. Gould, J. Opt. Soc. Am. B **2**, 1799 (1985).

[9] M. Kozuma, L. Deng, E. W. Hagley, J. Wen, R. Lutwak, K. Helmerson, S. L. Rolston, and W. D. Phillips, Phys. Rev. Lett. **82**, 871 (1999).

[10] P. J. Martin, B. G. Oldaker, A. H. Miklich, and D. E. Pritchard, Phys. Rev. Lett. **60**, 515 (1988).

[11] D. M. Giltner, R. W. McGowan, and S. A. Lee, Phys. Rev. A **52**, 3966 (1995).

[12] E. L. Bolda and D. F. Walls, Phys. Rev. Lett. **81**, 5477 (1998).

[13] E. M. Rasel, M. K. Oberthaler, H. Batelaan, J. Schmiedmayer, and A. Zeilinger, Phys. Rev. Lett. **75**, 2633 (1995).

[14] D. M. Giltner, R. W. McGowan, and S. A. Lee, Phys. Rev. Lett. **75**, 2638 (1995).

[15] A detailed discussion of the coherence properties of released BECs can be found in E. W. Hagley, Phys. Rev. Lett. (to be published). Because the momentum spread of a released BEC is much smaller than a photon recoil momentum, we neglect this spread in the treatment that follows.

[16] *Elements of Quantum Optics*, edited by P. Meystre and M. Sargent, 3rd ed. (Springer-Verlag, Berlin, 1998).

[17] M.-O. Mewes, M. R. Andrews, N. J. van Druten, D. M. Kurn, D. S. Durfee, and W. Ketterle, Phys. Rev. Lett. **77**, 416 (1996).

[18] U. Ernst, A. Marte, F. Schreck, J. Schuster, and G. Rempe, Europhys. Lett. **41**, 1 (1998).

[19] C. J. Myatt, N. R. Newbury, R. W. Ghrist, S. Loutzenhiser, and C. E. Wieman, Opt. Lett. **21**, 290 (1996).

[20] C. K. Law and N. P. Bigelow, Phys. Rev. A **58**, 4791 (1998).

[21] S. Inouye, A. P. Chikkatur, D. M. Stamper-Kurn, J. Stenger, D. E. Pritchard, and W. Ketterle, Science **285**, 571 (1999).

[22] Mikio Kozuma, Yoshio Torii, Toshiak Sugiura, Takahiro Kuga, E. W. Hagley, and L. Deng, Science **286**, 2309 (1999).